Council on Tall Buildings and Urban Habitat Korea

International Journal of
High-Rise Buildings
www.ctbuh-korea.org/ijhrb/index.php

International Journal of High-Rise Buildings
March 2024, Vol 13, No 1, 85-95
https://doi.org/10.21022/IJHRB.2024.13.1.85

Fire Behavior of Reinforced Concrete Filled Square Steel Tube Columns Under Constant Axial Loads

Jeeyoung Lee[1], Seulgi Han[2], Jinwon Shin[3], Inrak Choi[4], and Sungmo Choi[2†]

[1]*Department of Architectural Engineering, Urban Sciences of the University of Seoul, Korea*
[2]*Department of Architectural Engineering, University of Seoul, Korea*
[3]*Department of Architectural Engineering, Catholic Kwandong University, Korea*
[4]*Department of Civil Engineering, Hoseo University, Korea*

Abstract A composite member made of concrete-filled steel tubes (CFT columns) has been recognized for its fire resistance due to the thermal mass effect of concrete inside the steel tube, as shown in various studies. In this study, the fire resistance performance of reinforced CFT columns under constant axial load was evaluated using finite element analysis with ABAQUS. For this purpose, the variables including cross-section size, steel tube thickness, and concrete cover thickness were set, and the temperature distribution in the column cross-section exposed to a standard fire was investigated using heat transfer analysis. Ultimately, a P-M interaction curve was obtained by evaluating the overall residual strength of columns, and the fire resistance time was determined by evaluating axial displacement-time responses due to the reduction in load capacity during fire through stress analysis.

Keywords Reinforced Concrete-Filled Steel Tube, Heat Transfer Analysis, Stress Analysis, Compressive and Flexural Strength, Fire Resistance Performance

†Corresponding author:
Sung Mo Choi
E-mail: smc@uos.ac.kr

1. Introduction

In high-rise buildings, columns are the main vertical load-bearing members and should not only be able to resist lateral loads such as earthquakes and wind, but also include a certain amount of fire resistance to ensure that people have enough time to evacuate in the event of a fire. A concrete-filled steel tube column (CFT column) is a composite structure composed of a structural steel tube filled with concrete. The outer steel tube confines the concrete to restrain its lateral displacement, while the concrete retards the local buckling of the steel tube, enhancing the member's strength and ductility. Furthermore, due to the thermal storage effect of concrete in high-temperature fires, a certain level of fire resistance can be expected even without a fire resistance cover, unlike structural systems made of single materials. Additionally, since formwork is unnecessary and construction periods are shortened, the use of CFT columns is increasing across various construction sites due to their structural advantages and cost-effectiveness, and research on CFT columns is actively conducted worldwide.

In countries with advanced fire-resistant standards such as Europe, the United States, Japan, and Australia, performance-based structural of fire engineering design has been in practice for over two decades, and economic measures, such as reducing the thickness of the fire resistance cover or designing without a cover, are proposed based on the fire resistance performance of the CFT column itself. However, in Korea, regulations stipulate that the average temperature of the steel in each section should not exceed 538°C, and the temperature should not exceed 649°C at any place where the temperature is measured (KS F 2257-7:2019), and the same performance standards are provided for each type of major structural part based on the number of floors and maximum height depending on the use of the building(Regulations Concerning Standards for Evacuation and Fire Prevention Structures for Buildings). Specifically, columns are required to provide the fire resistance for 1 hour for buildings with less than 4 floors (20 m), 2 hours for those with less than 12 floors (50 m), and 3 hours for buildings above 12 floors (50 m), and the fire resistance performance should be secured by spraying and intumescent paint regardless of the performance of the member.

In this study, reinforcing bars were placed inside unprotected CFT columns to satisfy the fire resistance performance. The fire resistance of the column was evaluated when a certain central axial force was applied. For this purpose, the compressive and flexural strengths were

calculated according to the fire exposure time to obtain the P-M interaction curve, and numerical analysis was performed. Using a general-purpose finite element analysis program, ABAQUS (2023), heat transfer analysis was performed first to determine the temperature distribution of the CFT column cross-section during a fire, and thermal stress analysis was performed based on the heat transfer analysis results. To validate the analysis, the results of the numerical analysis were assess with the results of previous studies. In addition, a variable analysis was performed on the factors affecting the fire resistance performance for CFT columns to compare and analyze the fire resistance performance of each variable, including cross-section size, steel tube thickness, reinforcement ratio, concrete cover thickness, and axial force ratio.

2. Heat transfer

2.1. Analysis model

Table 1 shows the analytical matrix for this research. The selected specimens had a wide range of geometric, material and loading parameters. For each CFT specimen, Table 1 includes the cross-section size (b), steel tube thickness (t), column length (L), steel reinforcement details, steel yield strength (F_y), concrete compressive strength (f_c'), applied axial load (P_o) and the column end conditions (fixed or pinned). Columns numbered 7, 8, and 9 are noncompact composite sections, while the remaining columns are composite sections. The axial load capacity, P_o, referred in Table 1 was computed using Eq. (1) for compact composite sections, where A_s and A_c are the areas of the steel tube and concrete infill, respectively. P_o calculated by Eq. (1) was applied as the load of the column to check the fire resistance performance of the column in case of fire. The purpose of P_o is to determine fire resistance time by evaluating axial displacement-time responses resulting from the reduction in load capacity during a fire, using stress analysis. The axial displacement-time responses of CFT columns in the 0.4-0.5 axial force ratio range were compared and analyzed based on cross-section size and steel ratio, and the fire resistance time was measured. Although columns 7, 8, and 9 are noncompact sections, this study compares and analyzes within the 0.4-0.5 axial force ratio range, utilizing Eq. (1). To compare the fire resistance performance of CFT columns with and without reinforcement, columns numbered 4, 5, 6, 10, 11, 12, 16, 17, and 18 were left unreinforced for the study and the yield strength values of the steel tube, rebar, and concrete compressive strength were uniformly set to 355, 600, and 45, respectively.

$$P_0 = A_S F_y + A_{sr} F_{yr} + 0.85 A_c f_c' \quad (1)$$

A heat transfer analysis was conducted using ABAQUS, which is a commercially available nonlinear finite element analysis program. It simulates the heat transfer using a finite element formulation of the first variation of the basic energy balance equation along with the Fourier law

Table 1. Analytical matrix with CFT column specimen details

Column spec.	Cross-section dimensions $b \times b \times t$ (mm)	Length (mm)	Reinforcement no. × bar dia. (mm)	Yield strength, F_y (MPa)	Yield strength, F_{yr} (MPa)	Comp. strength, f_c' (MPa)	App. load, P_0(kN)	End cond.
1	400 × 400 × 9	6,500	8 × D25	355	600	45	12,681	pinned
2	400 × 400 × 9	6,500	16 × D29	355	600	45	16,177	pinned
3	400 × 400 × 9	6,500	16 × D32	355	600	45	17,542	pinned
4	400 × 400 × 12	6,500	-	355	-	45	11,725	pinned
5	400 × 400 × 16	6,500	-	355	-	45	13,385	pinned
6	400 × 400 × 19	6,500	-	355	-	45	14,559	pinned
7	600 × 600 × 9	6,500	24 × D19	355	600	45	24,207	pinned
8	600 × 600 × 9	6,500	24 × D29	355	600	45	29,006	pinned
9	600 × 600 × 9	6,500	28 × D32	355	600	45	32,837	pinned
10	600 × 600 × 12	6,500	-	355	-	45	22,416	pinned
11	600 × 600 × 16	6,500	-	355	-	45	25,089	pinned
12	600 × 600 × 19	6,500	-	355	-	45	27,023	pinned
13	800 × 800 × 16	6,500	28 × D29	355	600	45	49,958	pinned
14	800 × 800 × 16	6,500	28 × D35	355	600	45	54,900	pinned
15	800 × 800 × 16	6,500	36 × D35	355	600	45	59,199	pinned
16	800 × 800 × 22	6,500	-	355	-	45	45,181	pinned
17	800 × 800 × 25	6,500	-	355	-	45	47,757	pinned
18	800 × 800 × 28	6,500	-	355	-	45	50,274	pinned

of heat conduction. Three-dimensional (3D) finite element models were developed for conducting the heat transfer analyses of the CFT column specimens. The concrete infill and the steel tube were modeled using eight-node continuum (DC3D8) and four node shell (DS4) heat transfer elements, respectively.

The thermal boundary conditions of the simulation model were established by applying three different heat transfer mechanisms, namely conduction, convection, and radiation, to model the cross-section of the column exposed to fire. First, convection and radiation were uniformly applied to the entire fire area, and the convective heat transfer coefficient was 25 W/m^2·K, which is the recommended value for standard fire exposure conditions, for the heated surface according to EN 1991-1-2 (2002). Additionally, the emissivity of the steel tube was 0.7 in accordance with EN 1993-1-2 (2005). The absolute zero temperature is –273.15ºC, and the Stefan-Boltzmann constant of 5.67×10^{-8}W/m^2·K^4 is used as the radiation boundary condition for the heated surface. In the event of a fire, various fire scenarios exhibit temperature changes over time. However, this study assumes the use of the standard fire curve presented in the ISO 834, which is commonly employed in experiments and analyses, is assumed to be uniform on all four sides of the CFT column, as shown in Figure 1.

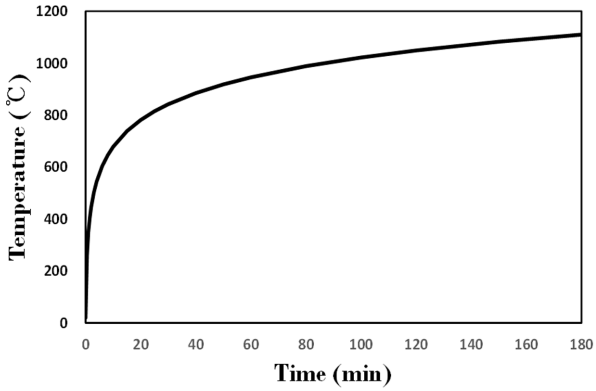


Figure 1. Standard fire curve (ISO 834)

2.2. Material thermal properties

The material thermal properties required for conducting the heat transfer analysis included the thermal conductivity and thermal capacity (specific heat multiplied by density), both of which could be temperature dependent. Table 2 provides the steel and concrete material thermal properties used in this research.

2.3. Validation of heat transfer analysis

To validate the thermal analysis results of the CFT column, temperature distributions at different depths of the 800 mm CFT column (column specimen 13) exposed to standard fire, based on Koo et al. (2013), were calculated. These calculated temperature distributions were then compared with those obtained through the ABAQUS thermal analysis. Figure 2 shows the relationship between temperature distribution and concrete depth according to the standard fire exposure time, as determined by heat

Table 2. Steel and concrete thermal properties at elevated temperatures

Steel				Concrete			
Temp. (ºC)	Thermal conductivity (J/s·m·ºC)	Thermal capacity (×10^6 J/m^3·ºC)	Thermal expansion (×10^{-6}/ºC)	Temp. (ºC)	Thermal conductivity (J/s·m·ºC)	Thermal capacity (×10^6 J/m^3·ºC)	Thermal expansion (×10^{-6}/ºC)
0	48.0	3.30	12.0	0	1.355	2.566	6.0
100	45.8	3.70	12.4	100	1.355	2.566	6.8
200	43.6	4.10	12.8	200	1.355	2.566	7.6
300	41.4	4.50	13.2	300	1.344	2.566	8.4
400	39.2	4.90	13.6	400	1.220	2.566	9.2
500	37.0	5.30	14.0	410	1.207	4.330	9.3
600	34.8	5.70	14.4	445	1.164	2.565	9.6
650	33.7	5.90	14.6	500	1.096	2.566	10.0
700	32.6	9.30	14.8	600	0.972	4.169	10.8
725	32.1	11.00	14.9	635	0.928	4.730	11.1
800	30.4	4.55	15.2	700	0.848	15.543	11.6
900	28.2	4.55	15.6	715	0.829	18.038	11.7
1000	28.2	4.55	16.0	785	0.742	2.565	12.3
				800	0.723	2.566	12.4
				900	0.599	2.566	13.2
				1000	0.475	2.566	14.0

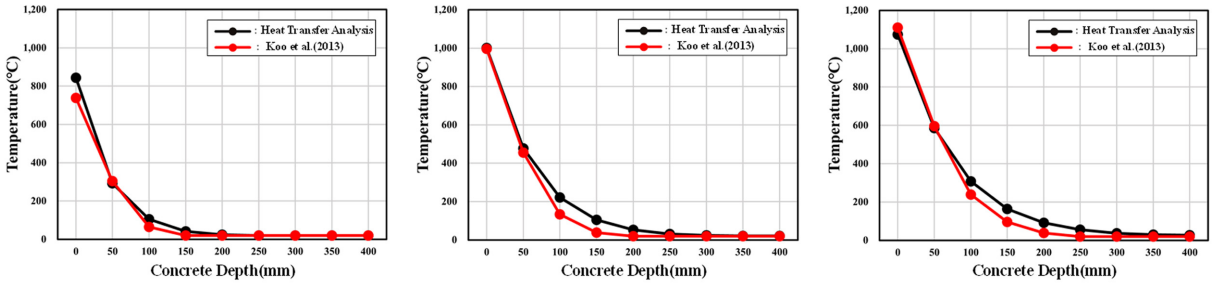


Figure 2. Comparison of heat transfer analysis and prior research (column specimen 13).

transfer analysis and Koo et al. (2013). The first value on the left side of each graph indicates the temperature of the steel tube, while the calculated value of Koo et al. (2013) used the average value of the inner and outer surface temperatures. It can be seen that for all fire exposure times, the Koo et al. (2013) predictions and the heat transfer calculations from this study and the temperature distribution by heat transfer analysis show a similar trend, with differences of less than 10%.

2.4. Heat transfer analysis results

2.4.1. Cross-section size

The temperature distribution of CFT columns exposed to a standard fire was compared by cross-section sizes. The graph in Figure 3 shows the temperatures measured at five different locations on a column with cross-section sizes of 400, 600, and 800 mm. The time-temperature curves of both the steel tube surface (point 1) and the rebar located 30 mm away from the inner surface of the steel tube (points 2 and 3) exhibited similar patterns regardless of the cross-section size. At the 1/4 point of the column (point 4), the temperature increased to 381°C for the 400 × 400 × 16 column, 189°C for the 600 × 600 × 16 column, and 84°C for the 800 × 800 × 16 column after 3 hours of heating. Figure 4 shows the temperature distribution after 3 hours of heating by cross-section size. As shown in Figure 4, following the 3 hours of heating, the concrete temperature of the 400 × 400 × 16 column remained below 200°C for only 6% of the total concrete area. In contrast, for the 600 × 600 × 16 column, this value was 35%, and for the 800 × 800 × 16 column, it reached 50%. This indicates that the temperature of the concrete decreased as the cross-section size increased. The temperatures at the centers of the columns did not exceed 200°C until the analysis was concluded.

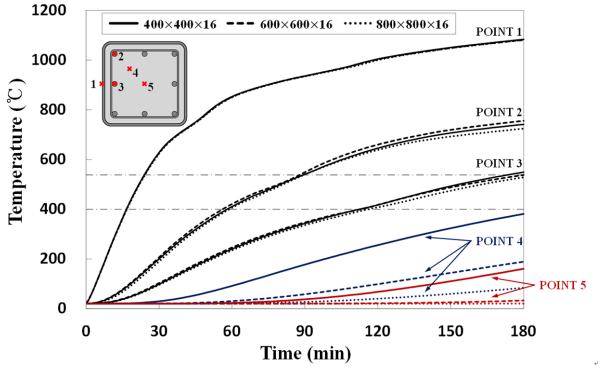


Figure 3. Time-Temperature curve as a function of cross-section size.

2.4.2. Steel tube thickness

The temperature distribution of CFT columns exposed to a standard fire was compared by the thickness of the steel tube. Figure 5 shows the temperature histories measured at four different locations with steel tube thicknesses of 9, 16, and 25 mm, on a column with a cross-section size of 600 mm. During the initial hour, the temperature of the steel tube increased rapidly, reaching 800°C, and the temperature rise was slower as the

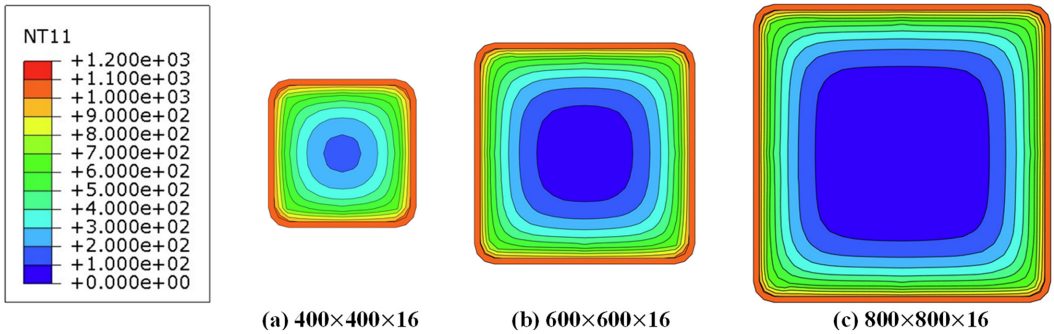


Figure 4. Temperature distribution of section as a function of cross-section size.

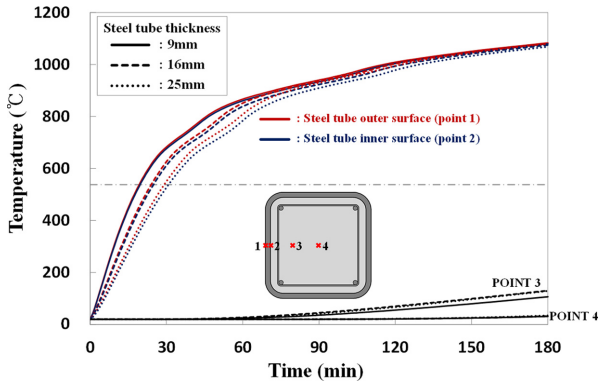


Figure 5. Time-Temperature curve as a function of steel tube thickness

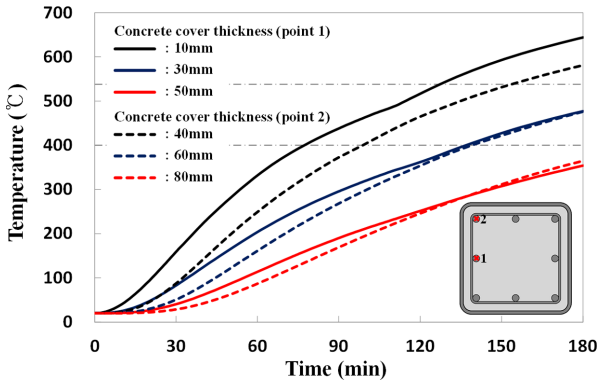


Figure 7. Time-Temperature curve as a function of concrete cover thickness

thickness of steel tube increased. At 15 minutes, the temperature of the 9 mm steel tube was up to 164°C higher than that of the 25 mm steel tube. However, after the steel tube temperatures reached 900°C at approximately 75 minutes, their temperatures became similar and reached over 1,000°C after 3 hours. The temperature difference between the outer (point 1) and the inner surface (point 2) of the steel tube is negligible for a steel tube thickness of 9 mm. However, for a thickness of 16 mm, a difference of roughly 15°C is observed between 20 and 100 minutes, and for a thickness of 25 mm, the difference is approximately 25°C, and gradually decreases over time. The temperatures of concrete at the points 3 and 4 were analyzed to be insignificant due to the variation in steel tube thickness. Figure 6 shows the temperature distribution after 3 hours of heating by steel tube thickness.

2.4.3. Concrete cover thickness

The thickness of concrete cover is the distance from the inside face of the steel tube to the outer surface of the rebar. The temperature of the rebar exposed to a standard fire was compared by the concrete cover thickness. Figure 7 shows the time-temperature curves of the rebars located at the center of the CFT column side and at the corner according to the concrete cover thickness. After 1 hour of heating with standard fire, the temperature of the side rebar was 332, 204, and 114°C for concrete cover thicknesses of 10, 30, and 50 mm, respectively, decreasing with increasing concrete cover thickness. After 2 hours of exposure to the standard fire, the temperatures were 517, 362, and 252°C for concrete cover thicknesses of 10, 30, and 50 mm, respectively. These temperatures were 185, 158, and 138°C higher than those observed after 1 hour exposure to the standard fire, indicating that the rate of temperature increase decreased as the concrete cover thickness increased. Furthermore, when exposed to the standard fire for 3 hours, the temperatures were 644, 478, and 354°C. It was observed that when the concrete cover thickness increased to 30 mm or more, the temperature remained below the critical temperature of 538°C. Similarly, for the rebar located at the corner, when exposed to the standard fire for 3 hours, the temperatures were measured at 582, 477, and 365°C corresponding to concrete cover thicknesses of 40, 60, and 80 mm, respectively, with the temperature decreasing as the concrete cover thickness increased. It was found that the temperature remained below the critical temperature of 538°C when the concrete cover thickness increased beyond 60 mm.

The temperature of the rebar decreased with increasing concrete cover thickness. The rebar located at the center of the CFT column side remained below the critical temperature of 538°C at a concrete cover thickness of 30 mm. For hot-rolled steel bars, strength calculations could be performed without any reduction in material yield strength up to 400°C. This temperature remained

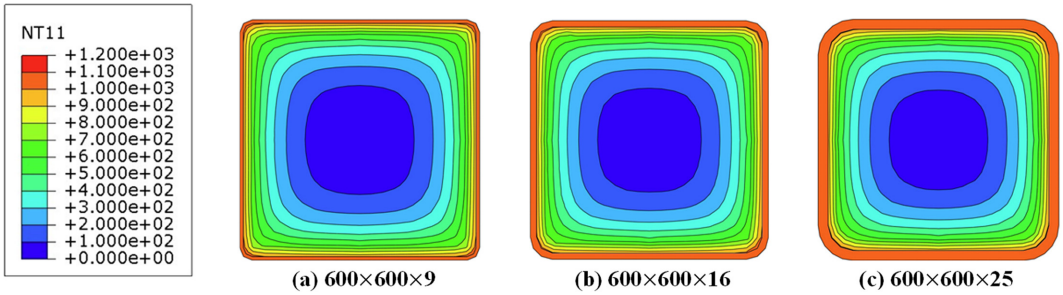


Figure 6. Temperature distribution of section as a function of steel tube thickness.

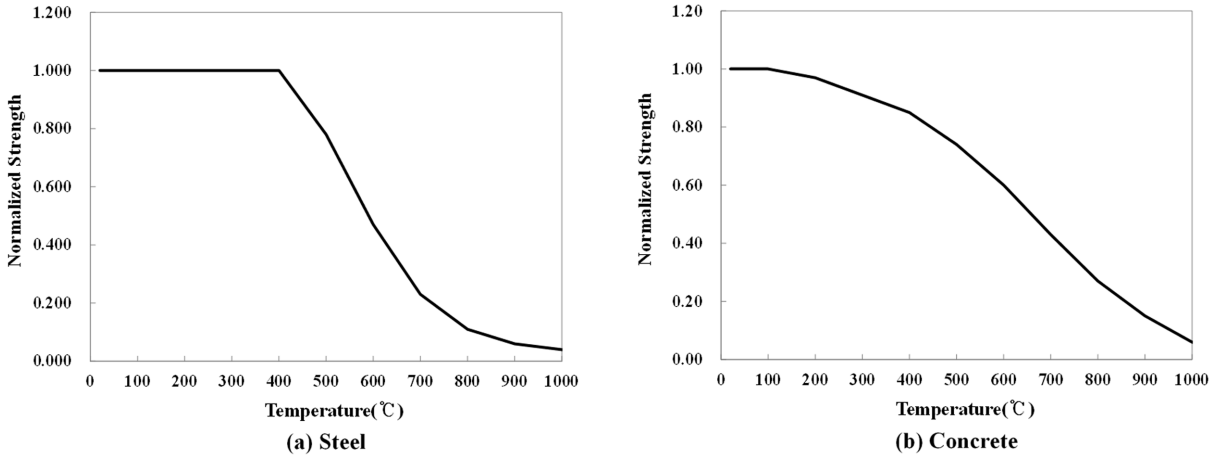


Figure 8. Normalized strength of steel and concrete as a function of temperature

below 400°C as the concrete cover thickness increased to 50 mm or more. On the other hand, the rebar located at the corners of the CFT column was exposed to heat in both directions, and the temperature was about 200°C higher than that of the rebar located at the center of the column side with the same concrete cover thickness. This temperature was maintained below the critical temperature of 538°C at a concrete cover thickness of 60 mm, and below 400°C when the concrete cover thickness increased to 80 mm or more.

3. Evaluation of Fire Resistance Performance

3.1. Strength reduction factor of increasing temperature

The strength reduction factor of steel and concrete with increasing temperature is shown in Figure 8. Structural steels show no reduction in yield strength up to 400°C and retain only 23% of their room temperature strength at 700°C. At 800°C, the strength decreases to 11%, and at 900°C, it decreases to 6%. Based on the temperature distribution results of the column cross-section at a specific fire time obtained through heat transfer analysis, strength reduction factors were applied to the steel tube, rebar, and concrete of the CFT column. It was observed that applying a concrete cover thickness of 80 mm for the rebar located at the corners and 50 mm for the rebar located at the center of the column side does not reduce the yield strength of the rebar when exposed to a standard fire for 3 hours. To investigate the compressive and flexural performance of the column under fire conditions, when the rebar is placed inside the column so that it is less affected by fire, the compressive and flexural strengths were evaluated by considering the strength reduction factor due to the temperature increase of the steel tube, rebar, and concrete of the CFT column exposed to a standard fire, and the P-M interaction curve was constructed according to KDS 14 31 00:2017.

3.2. P-M interaction curve

The fire resistance performance was evaluated when reducing the steel tube thickness of the unreinforced CFT column and replacing that steel with an equivalent amount of rebar. The compressive and flexural strengths for 3 hours of exposure to a standard fire are shown in Table 3, and the corresponding P-M interaction curves are shown in Figure 9.

Table 3. Compressive and flexural strength of CFT columns after 3 hours of fire heating

Column spec.	Steel tube area A_s(mm^2)	Reinforcement area A_{sr}(mm^2)	Steel ratio	Concrete cover (mm)	Room temperature		After 3 hours		$\frac{P_{n,fi}}{P_n}$	$\frac{M_{n,fi}}{M_n}$
					P_n (kN)	M_n (kN·m)	$P_{n,fi}$ (kN)	$M_{n,fi}$ (kN·m)		
5	23,260	0	0.148	-	10,885	1,076	1,209	25	0.11	0.02
2-1	13,630	10,278	0.150	0	12,605	1,447	1,415	66	0.11	0.05
2-2	13,630	10,278	0.150	50/80	11,913	1,226	5,002	549	0.42	0.45
11	36,060	0	0.101	-	22,555	2,699	4,255	35	0.19	0.01
8-1	20,860	15,417	0.101	0	25,570	3,496	4,807	147	0.19	0.04
8-2	20,860	15,417	0.101	50/80	25,105	3,162	14,455	1514	0.58	0.48
18	82,430	0	0.130	-	47,636	7,844	12,457	84	0.26	0.01
15-1	48,860	34,437	0.130	0	55,531	10,431	13,643	425	0.25	0.04
15-2	48,860	34,437	0.130	50/80	55,159	9,682	34,408	4,733	0.62	0.49

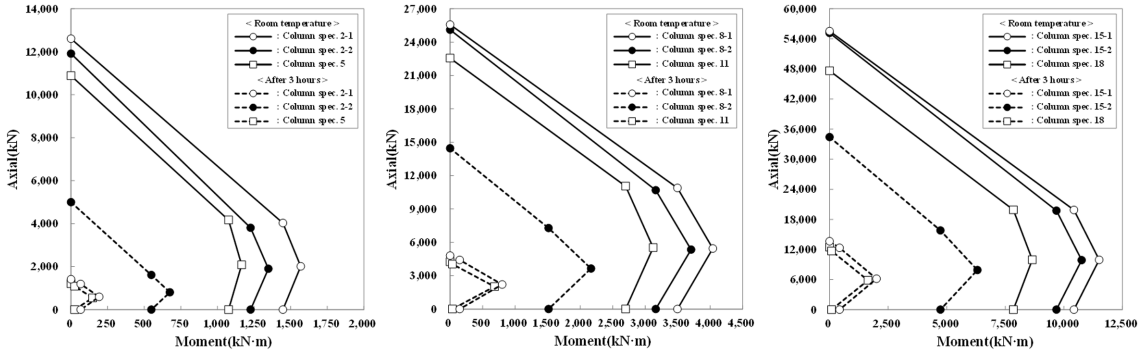


Figure 9. P-M interaction curve of CFT columns after 3 hours of fire heating

The compressive and flexural strengths of a CFT column with a section size of 400 × 400 mm and a steel tube thickness of 16 mm were compared to those of a CFT column with the same 400 × 400 mm section size but with the steel tube thickness reduced to 9 mm and reinforced with 16 × D29 rebars. The steel ratio remains the same at about 0.15 by reinforcing with rebar as much as the thickness of the steel tube is reduced. If it's reinforced, the compressive and flexural strengths were compared at room temperature and after 3 hours of exposure to a standard fire when the rebar was placed without a concrete cover thickness, and the rebar at the corner placed with 80 mm concrete cover thickness and the rebar at the column side placed with 50 mm concrete cover thickness. After 3 hours of exposure to the standard fire, the compressive strengths of specimens 5, 2-1 and 2-2 decreased by 89, 89, and 58%, respectively, compared to the compressive strength at room temperature, and the flexural strength decreased by 98, 95, and 55%, respectively, compared to the flexural strength at room temperature. The unreinforced CFT columns showed a severe decrease in strength due to the loss of steel tubes as the steel tubes rose to over 1000°C after 3 hours of exposure to fire, and even if the reinforcement was reinforced, the strength was significantly reduced due to the significant temperature rise when the reinforcement was located close to the fire exposure surface, resulting in a decrease in strength compared to the concrete cover thickness of 50 and 80 mm.

Similarly, the compressive and flexural strengths of a CFT column with a section size of 600 × 600 mm and a steel tube thickness of 16mm were compared to those of a CFT column with the same 600 × 600 mm section size but with the steel tube thickness reduced to 9 mm and reinforced with 24 × D29 rebars along the thickness of the concrete cover. The steel ratio remains the same at about 0.101. After 3 hours of exposure to the standard fire, the compressive strength decreased by 81, 81, and 42% compared to the compressive strength at room temperature, and the flexural strength decreased by 99, 96, and 52% compared to the flexural strength at room temperature (column specimen 11, column specimen 8-1, and column specimen 8-2).

The same method was used to compare the compressive and flexural strengths of a column with a cross-sectional size of 800 × 800 mm exposed to a standard fire. After 3 hours of exposure to the standard fire, the compressive strength decreased by 74, 75, and 38% compared to the compressive strength at room temperature, and the flexural strength decreased by 99, 96, and 51% compared to the flexural strength at room temperature (column specimen 18, column specimen 15-1, and column specimen 15-2).

The compressive and flexural performance at elevated temperatures were improved when the temperature rise of the rebar was suppressed by placing the rebar inward of concrete. In addition, the residual performance improved as the section size increased, but the residual compressive performance was up to 26% and the residual flexural performance was 5% in the case of no reinforcement and no concrete cover thickness, while the residual compressive performance and residual flexural performance increased up to 62% and 49% with the concrete cover thickness. Reducing the thickness of the steel tube and replacing it with rebar by the same amount of steel was found to have a more favorable effect on the fire resistance performance.

3.3. Stress analysis

3.3.1. Analysis model

The nonlinear stress analysis was also conducted using ABAQUS, which provides the option for sequential heat transfer and stress analysis. The nonlinear stress analysis was conducted to determine the complete structural responses of CFT column specimens subjected to combine axial and thermal loading. The thermal loading was obtained from results of heat transfer analysis. The concrete infill and the steel tube were modeled using eight-node continuum (C3D8R) and four node shell elements (S4R) with reduced integration, respectively. The longitudinal steel reinforcement was modeled using two node truss elements (T3D2) that were embedded in the concrete elements.

The contact between the surface of the steel tube and the concrete infill is modeled using a surface-to-surface contact. The thermal resistance at the boundary between the steel tube and the concrete core was modeled using a

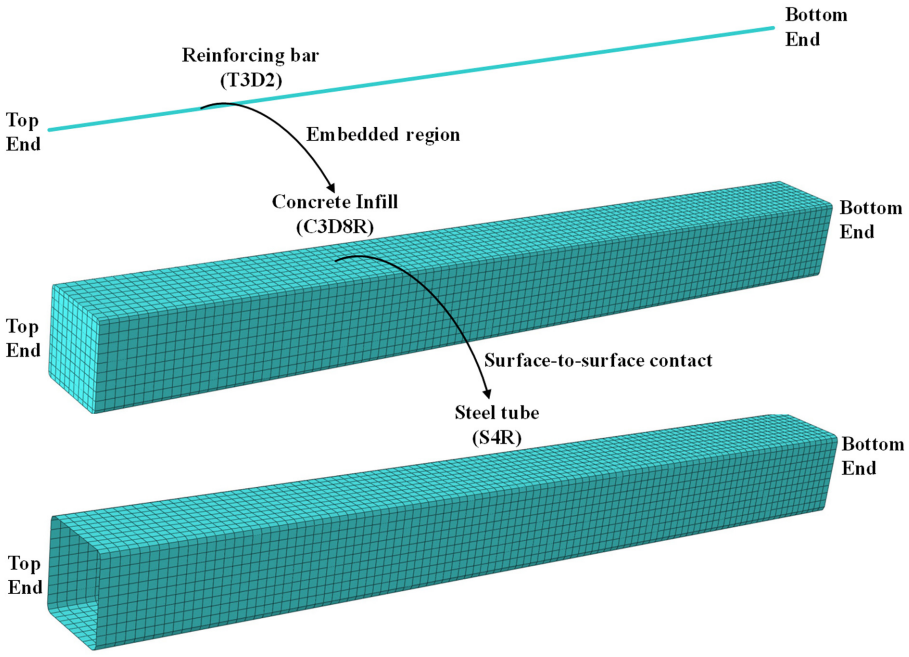


Figure 10. 3D finite element model for CFT column specimens.

constant value of 200 W/m^{2}K for the gap conductance according to Espinos A, Et al. (2010). The mechanical interaction between the steel tube and concrete infill contacting surfaces was modeled as follows. The normal behavior employed a "hard point" contact formulation, which allows for any pressure value when the surfaces are in contact and transmits no pressure when the surfaces do not contact. The tangent behavior was modeled using the Coulomb friction with a constant friction coefficient of 0.3.

Figure 10 shows examples of the 3D finite element models developed using ABAQUS. The 3D finite element models were subjected to axial loading first. The axial loads were maintained constant while applying thermal loading. The results from the finite element analyses included the 3D deformations, strains, and stresses histories for the CFT columns.

3.3.2. Validation of stress analysis

To validate the stress analysis results of the CFT column, axial displacement-time ($\delta-$t) response was calculated based on Hong S, Varma AH. (2009) in Table 4. The $\delta-$t response was then compared with the result obtained through ABAQUS stress analysis as shown in Figure 11. The graphical comparisons of Figure 11 indicate that the numerical models predict the trends of prior research's measurement $\delta-$t response reasonably but with some discrepancies. These discrepancies are caused by the several assumptions and limitations of the numerical models. Material behavior at elevated temperatures can exhibit significant variability and uncertainty, and the authors did not provide all the necessary material measurements to validate the assumed models. Stress analysis and Hong S, Varma AH. (2009) failure times are indicated by solid circles (grey dots) in the Figure 11 and was equal to 150 min. In this chapter, the objective is to determine the failure time of CFT columns. Despite the assumptions, limitations, and potential errors, it has been confirmed that stress analysis predicts failure times with reasonable accuracy.

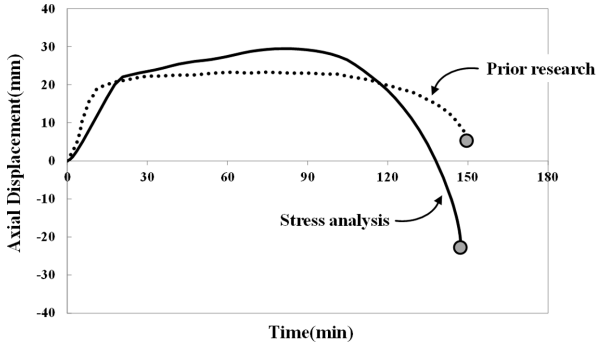


Figure 11. Comparison of stress analysis and prior research's δ-t curve

Table 4. CFT column details from Hong S, Varma AH. (2009)

Cross-section dimensions $b \times b \times t$ (mm)	Length (mm)	Reinforcement no.×bar dia. (mm)	Yield stress Fy (MPa)	Yield stress Fyr (MPa)	Comp. stress f_c' (MPa)	App. load P_0(kN)	$\frac{P}{P_0}$	$\frac{KL}{r}$	End cond.
203 × 203 × 6.35	3,810	4 × D16	350	600	47	500	16	28.1	pinned

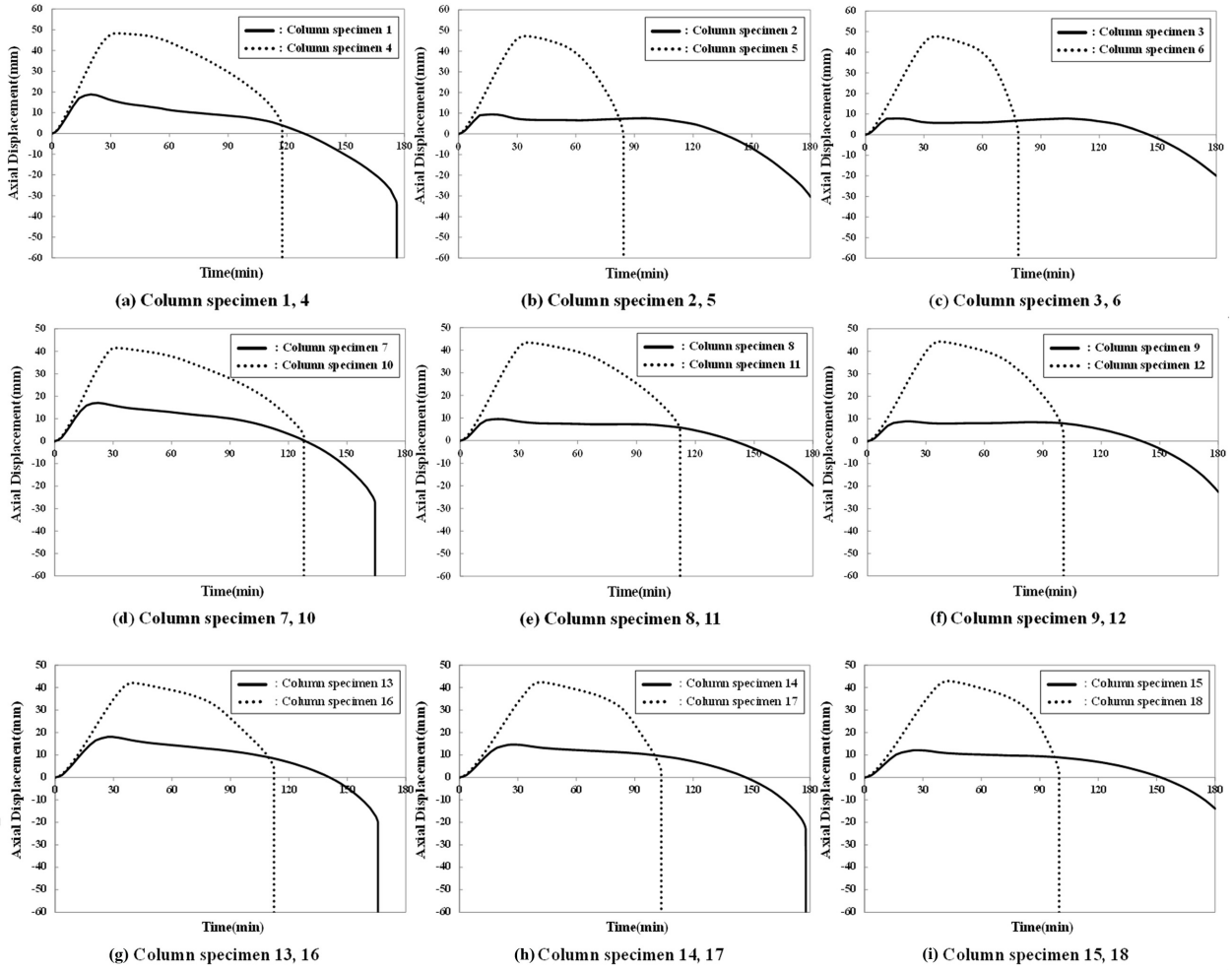


Figure 12. Axial displacement with standard fire exposure time.

3.3.3. Axial displacement

The axial displacement-time responses of the CFT columns due to the reduction in load capacity during the fire were evaluated, as shown in Figure 12. The axial displacement-time responses of CFT columns in the 0.4-0.5 axial force ratio range were compared and analyzed based on cross-section size and steel ratio, and the fire resistance time was measured. Figure 12 compares the axial displacement-time responses of standard CFT columns with reinforced CFT columns that have the same steel ratio by reducing the thickness of the steel tube in the CFT column and reinforcing it with rebars inside the concrete. Variable interpretation and these failure times are provided in Table 5. In the case of standard CFT columns, after sufficient thermal expansion of the steel tube, the concrete experienced shrinkage displacement. However, this was insufficient to produce the necessary axial displacement, leading to sudden failure at some point. In contrast, the reinforced CFT columns exhibited slower development of axial shrinkage displacement at the same axial force ratio and demonstrated higher fire resistance performance compared to the unreinforced ones before eventually failing. The time it takes for the CFT column to reach its maximum expansion point is influenced by the steel tube. It can be observed that after a rapid axial contraction, the rate of axial compressive displacement decreases as the cross-section size increases. Larger cross-section sizes are associated with greater fire resistance times. Regardless of the section size and steel ratio, when the steel ratio is the same, the fire resistance time is greater when reinforced. Specifically, the fire resistance performance reaches 3 hours for 400 × 400 mm sections and 4% rebar ratio, and 600 × 600 and 800 × 800 mm sections result in a 3-hour fire resistance performance for 6% rebar ratio, while standard CFT columns do not meet the 3-hour fire resistance.

4. Conclusions

An analytical approach consisting of sequentially coupled analysis steps, heat transfer analysis and stress analysis, was used to predict the behavior of the reinforced CFT columns subjected to standard fire loading. The heat transfer and stress analyses were conducted

Table 5. Numerical predictions for CFT column specimens

Column spec.	Cross-section dimensions $b \times b \times t$ (mm)	Reinforcement no.×bar dia. (mm)	Steel ratio	Concrete cover (mm)	App. Load P (kN)	$\frac{P}{P_0}$	Failure time (min)
1	400 × 400 × 9	8 × D25	0.112	50/80	5,072	0.4	176
4	400 × 400 × 12	-	0.112	-	4,690	0.4	117
2	400 × 400 × 9	16 × D29	0.148	50/80	8,089	0.5	180
5	400 × 400 × 16	-	0.150	-	6,693	0.5	84
3	400 × 400 × 9	16 × D32	0.166	50/80	8,771	0.5	180
6	400 × 400 × 19	-	0.173	-	7,280	0.5	78
7	600 × 600 × 9	24 × D19	0.077	50/80	12,104	0.5	164
10	600 × 600 × 12	-	0.077	-	11,208	0.5	127
8	600 × 600 × 9	24 × D29	0.101	50/80	14,503	0.5	180
11	600 × 600 × 16	-	0.101	-	12,545	0.5	112
9	600 × 600 × 9	28 × D32	0.119	50/80	16,419	0.5	180
12	600 × 600 × 19	-	0.119	-	13,512	0.5	100
13	800 × 800 × 16	28 × D29	0.104	50/80	24,979	0.5	165
16	800 × 800 × 22	-	0.104	-	22,591	0.5	112
14	800 × 800 × 16	28 × D35	0.118	50/80	27,450	0.5	177
17	800 × 800 × 25	-	0.118	-	23,879	0.5	103
15	800 × 800 × 16	36 × D35	0.130	50/80	29,600	0.5	180
18	800 × 800 × 28	-	0.130	-	25,137	0.5	99

using the 3D finite element with ABAQUS. The variables, including cross-section size, steel tube thickness, and concrete cover thickness, were set, and the temperature distribution in the CFT column cross-section exposed to a standard fire was investigated using heat transfer analysis. The P-M interaction curve was obtained by evaluating the overall residual strength of columns, and the fire resistance time was determined by evaluating axial displacement-time responses due to the reduction in load capacity during fire through stress analysis. The following significant conclusions are drawn from this paper:

1. The temperature of the concrete exposed to a standard fire decreased as the cross-section size increased. The temperature of the steel tube exposed to a standard fire increased rapidly, reaching 800ºC within 1 hour, with the temperature rise slowing down as the thickness of steel tube increased.
2. The temperature of the rebar located at the CFT column side remained below 400°C at a concrete cover thickness of 50 mm, and the rebar located at the corner remained below 400°C at a concrete cover thickness of 80 mm.
3. The residual compressive and flexural performance were improved when the temperature rise of the rebar was suppressed by placing it inward of concrete and reducing the thickness of the steel tube and replacing it with an equivalent amount of rebar was found to have a more favorable effect on the fire residual performance.
4. The numerical predictions derived from axial displacement-time responses through stress analysis shows that the reinforced CFT columns exhibited slower development of axial shrinkage displacement at the same axial force ratio and demonstrated higher fire resistance performance, reaches 3 hours, compared to the unreinforced ones.

In the future, reinforcing CFT columns with rebar inside the concrete can be considered a means to secure fire resistance performance in high-rise buildings without the need for a fire resistance cover.

Acknowledgments

A short section may acknowledge assistance and sources of financial support.

References

Choi, I. R. (2020). “High-Temperature Thermal Properties of Sprayed and Infill-Type Fire-Resistant Materials Used in Steel-Tube Columns.” *International Journal of Steel Structures*, Vol.20, No.3, 777-787

Cho, K. S. (2011). “An Experimental Study on the Fire Resistance Performance of the Reinforced Concrete Columns According to the Cross Section Size and Depth of Concrete Cover.” J*ournal of Korean Institute of Fire Sci & Eng*., Vol.25, No.1, 78-84.

EN 1991-1-2 (2002). “Eurocode 1: Actions on Structures –

Part 1-2: General Actions - Actions on Structures Exposed to Fire." European Committee for Standardization.

EN 1993-1-2 (2015). "Eurocode 3: Design of Steel Structures – Part 1-2: General Rules – Structural Fire Design." European Committee for Standardization.

EN 1994-1-2 (2005). "Eurocode 4: Design of Composite Steel and Concrete Structures – Part 1-2: General Rules – Structural Fire Design." *European Committee for Standardization.*

Espinos, A. Et al. (2010). "Advanced model for predicting the fire response of concrete filled tubular columns." *Journal of Constructional Steel Research*, 66(8), 1030-1046.

Han, S. G. Et al. (2022). "Evaluation of Fire Resistance of Concrete Filled Steel Tube Column by Spray-Applied Fire Resistive Material and CFRP Re-Bar Internal Arrangement." *Journal of the Korean Society for Advanced Composite Structures*, Vol.13, No.5, 37-47.

Han, S. G. Et al. (2023). "Flexural Performance of Concrete-Filled Composite Beams with Carbon Fiber-Reinforced Plastic Rebar Exposed to Standard Fires." *Journal of the Korean Society for Advanced Composite Structures*, Vol.14, No.1, 17-27.

Han, S. G. Et al. (2023). "Compressive and Flexural Performance of Concrete Columns Reinforced with Steel/ CFRP Re-bars Exposed to 3 Hours Standard Fire." *Journal of the Korean Society for Advanced Composite Structures*, Vol.14, No.3, 1-12.

Hong, S., and Varma, A. H. (2009). "Analytical modeling of the standard fire behavior of loaded CFT columns." Journal of Constructional Steel Research, Vol.65, No.1, 54-69.

Kim, S. H. (2012). "A Study on the Evaluation of Residual Strength of Double Concrete Filled Tube Column by Unstressed test." *Journal of Korean Society of Steel Construction*, Vol.24, No.1, 88-89.

Kim, S. H. (2014). "Improving Structural and Fire Performance with Steel-Fibers for Internally Anchored Square Composite Columns." *Doctoral Dissertation, Depart-ment of Architectural Engineering*, University of Seoul, Seoul, Korea.

Kim, S. H., and Yom, K. S. (2017). "Evaluation of Resistance Strength and Behavior of Reinforced STG 800 Welded Square Composite Column after Fire 3 Hour." *2021 Proceedings of the Korean Institute of Building Construction Conference*, Seoul, Korea, 242-243.

KS F 2257-1 (2019). "Methods Fire Resistance Test for Elements of Building Construction-General Requirements." *Korean Agency for Technology and Standards (KS)*, Seoul, Korea.

KS F 2257-7 (2019). "Methods of Fire Resistance Test for Elements of Building Construction- Specific Requirements for Columns." *Korean Agency for Technology and Standards (KS)*, Seoul, Korea.

Lee, C. R. (2021). "A Study on Mathematical Evaluation of the Fire Resistance Performance for Reinforced Concrete Filled Steel Tube Columns." *Master Thesis, Department of Architectural Engineering*, Urban Sciences of the University of Seoul, Seoul, Korea.

Lee, J. Y. (2023). "Compressive and Flexural Strength of Reinforced Concrete Filled Square Steel Tube Columns Exposed to Standard Fire." *Master Thesis, Department of Architectural Engineering*, Urban Sciences of the University of Seoul, Seoul, Korea.

Park, S. H. Et al. (2007). "An Evaluation for the Fire Resistance of Concrete-Filled Steel Sq*uare Tube Columns under Constant Axial Loads." Journal of Korean Society of Steel Construction*, Vol.19, No.6, 703-714.

Song, K. C. (2010). "A Study on the Evaluation Fire-resistance Capacities for Advanced Square CFT Columns." *Master Thesis, Department of Architectural Engineering*, University of Seoul, Seoul, Korea.

Wang, Y. C. (2005). "Steel and Composite Structures Behavior and design for fire safety." *Taylor & Francis Group.d*